Materials Science & Engineering A 731 (2018) 29–35

Contents lists available at ScienceDirect

Materials Science & Engineering A

journal homepage: www.elsevier.com/locate/msea

Mechanical properties of an aged Ni-Cr-Mo alloy and effect of long-range order phase on deformation behavior

Wanjun He*, Rui Hu, Yang Wu, Xiangyu Gao, Jieren Yang

State Key Laboratory of Solidification Processing, Northwestern Polytechnical University, Xi'an 710072, China

ARTICLE INFO

Keywords:
Ni-Cr-Mo alloy
Aging treatment
Long-range order phase
Strain hardening
Mechanical twinning

ABSTRACT

Mechanical properties of a Ni-Cr-Mo alloy subjected to an aging treatment at 600 °C and effect of long-range order (LRO) phase on deformation behavior of the alloy are systematically investigated. Results show that peak-aging conditions are reached after 600 h of aging at 600 °C. Meanwhile, the aging treatment at 600 °C in the aging time range of 100–700 h can lead to the precipitation of the coherent Pt_2Mo-type LRO phase in the C2000 alloy. Fine scale Pt_2Mo-type LRO phase exists in the sample aged for 100 h and provides an enhanced yield strength. Because the solution treated sample and the sample aged for 100 h show the almost identical strain hardening behaviors, it can be suggested that the ordered structure of the fine scale LRO phase is destroyed during the quite small plastic deformation. Besides, the ordered structure of the relatively large LRO phase is destroyed after the large deformation. Mechanical twinning occurs in the tensile-failed sample which is aged for 500 h. And, mechanical twinning is responsible for the high ductility of the alloy aged for more than 100 h and the change in the shape of the strain hardening rate *vs* true strain curve.

1. Introduction

Hastelloy C2000 alloy, with a nominal composition of Ni-23Cr-16Mo (wt%), can resist a wide variety of aggressive chemicals and is used in a range of industrial applications [1–3]. The superalloy based on the Ni–Cr–Mo ternary system is a very significant class of superalloy using superlattice phase (i.e., long-range order (LRO) phase) as a primary strengthening mechanism [4,5]. For instance, the yield strength of the aged commercial HAYNES® 242™ alloy (Ni–25Mo–8Cr, wt%), is twice greater than that of the solution treated alloy [6,7]. And, the yield strength and ultimate tensile strength of the aged HAYNES® 242™ alloy increase with the increasing size of Pt_2Mo-type LRO phase [4]. However, it is reported that the yield strength and ultimate tensile strength of aged C-22HS (Ni–21Cr–17Mo, wt%) alloy decrease with the increasing size of Pt_2Mo-type LRO phase but increase with the increasing volume fraction of the phase [8]. Besides, widespread mechanical twins are observed in the tensile-tested sample of the aged C-22HS alloy [9]. Our previous work [10,11] has proposed that Pt_2Mo-type LRO phase can precipitate in the C2000 alloy during an aging treatment at 600 °C in the aging time range of 100–500 h and has demonstrated that the LRO phase is identified as being $Ni_2(Cr,Mo)$ stoichiometry. However, the effect of the aging time on the mechanical properties of the C2000 alloy remains unclear.

In this work, the mechanical properties of the C2000 alloy subjected to solution heat treatment followed by aging to various hours are investigated and discussed in relation to the effect of the LRO phase on deformation behavior of the alloy. This adds to existing literature data that refer mostly to the evolution behavior of the Pt_2Mo-type LRO phase in the C2000 alloy during aging treatment.

2. Materials and experimental procedures

The C2000 alloy studied in this work, with the chemical composition of Ni–22.66Cr–15.80Mo (wt%) with 1.53Cu, 0.75Fe, 0.24Al, 0.23Mn, 0.20Co, 0.02Si, 0.003 P, 0.001 S and 0.001 C as minority alloying elements, was received in a hot-rolled and annealed state by Haynes International Inc.,USA. The plate samples were cut from bulk materials using electro discharge machining (EDM). Then, these samples were solution treated at 1150 °C for 2 h and subsequently water quenched. Subsequently, the solution treated samples were aged at 600 °C for different hours (50 h, 100 h, 300 h, 500 h, 600 h, 700 h) and then air cooled to precipitate ordered phase in the alloy matrix.

After aging, the plate samples were cut into the tensile samples with a cross-section of $2 \times 2\ mm^2$ and a gauge length of 14 mm, as shown in Fig. 1. The uniaxial tensile tests were performed using an ASTM-E8M machine at room temperature with a constant strain rate of $10^{-3}\ s^{-1}$. Samples for optical microscopy (OM) were electrolytically polished using an electrolyte comprising 5% perchloric acid and 95% ethanol by

* Corresponding author.
E-mail address: hewanjun@mail.nwpu.edu.cn (W. He).

https://doi.org/10.1016/j.msea.2018.06.032
Received 30 March 2018; Received in revised form 5 May 2018; Accepted 7 June 2018

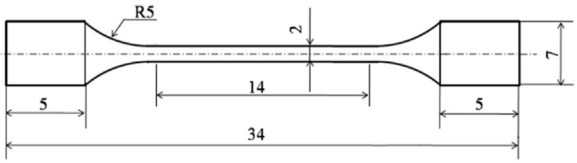

Fig. 1. Diagram of a tensile test sample.

volume and etched with a solution of 60% hydrochloric acid and 40% hydrogen peroxide by volume. Electron backscattered diffraction (EBSD) samples were also prepared with the electrolytic polishing. The transmission electron microscopy (TEM) thin foil specimens were first mechanically polished to a thickness of approximately 40–50 μm. Then, electropolishing was performed with a double-jet electropolishing device using an electrolyte comprising 20% perchloric acid and 80% ethanol by volume under a temperature of 253 K (− 20 °C). The TEM foils were observed using the bright-field (BF), dark-field (DF) and selected area electron diffraction (SAED) modes. The orientation relationship and interface structure between the LRO phase and the Ni-based matrix were studied by high resolution electron microscopy (HRTEM).

3. Results and discussion

3.1. Characterization of microstructure and LRO phase

Fig. 2a is a typical optical microstructure of the aged C2000 alloy and shows that the sample consists of equiaxed grains with an average size of 300 μm. And, there is no any type of secondary particle inside grain or at grain boundary. It should be mentioned that all different heat-treated samples (including solution treated sample and samples aged for different hours) are closely similar to each other in optical microstructures, implying that the transformation products during the aging treatment are too fine scale to be resolvable optically. The all Euler map (Fig. 2b) of the aged alloy shows that a large number of lamella-like straight annealing twins are present in the interior of the grains. This can be explained by the low stacking fault energy (SFE) of the experimental Ni-Cr-Mo alloy with a face-centered cubic structure [12].

The samples aged at 600 °C for 100 h, 500 h and 700 h are selected for detail analysis on the LRO phase. It should be mentioned the diffraction spots of the SAED patterns along [001] (or [$\bar{1}$12]) zone axes of the alloys aged for 100 h, 500 h and 700 h have the same distribution characteristics, i.e., their phase compositions are the same. Therefore, we choose only one sample, such as the sample aged for 700 h, for the analysis on the crystallographic and ordering characteristics of the LRO phase. Fig. 3a and b show the SAED patterns of the alloy aged at 600 °C for 700 h along [001] and [$\bar{1}$12] zone axes, respectively. A feature of the unit cell of the Pt_2Mo-type LRO phase with $Ni_2(Cr,Mo)$ stoichiometry is that every third {420} and {220} f.c.c. lattice planes are occupied by Cr/Mo atoms and the intervening planes are solely occupied by Ni atoms [8]. As a result, superlattice reflections of the Pt_2Mo-type LRO phase occur at every $\frac{1}{3}${420} and $\frac{1}{3}${220} positions in reciprocal space. This exactly coincides with the SAED pattern (Fig. 3a). Therefore, the three aforementioned samples can be confirmed to contain the Pt_2Mo-type LRO phases. It is known that the Pt_2Mo-type LRO phase has a body centered orthorhombic structure where six orientational variants can be directly derived from the parent f.c.c. lattice [13]. Therefore, as indicated in Fig. 3a, there are a pair of parallel twin variants in the [001] section. While in the [$\bar{1}$12] section, three twin variants which are in perpendicular orientation with each other are indicated by Fig. 3b. According to the superlattice reflections, the DF images of the three samples are obtained. Fig. 3c presents a DF image of the alloy aged for 100 h, where irregularly shaped Pt_2Mo-type LRO phases with an average size of approximately 10 nm are dispersedly distributed in the alloy matrix. However, as indicated in Fig. 3d, the average size of the LRO phase in the alloy aged for 500 h is approximately 40 nm, and the shape of the LRO phase is roughly spherical. With the aging time further increasing to 700 h, the average size of the LRO phase remains near 40 nm, but the distribution of the LRO phase is much denser (Fig. 3e). And, there are some particle coalescence behaviors in the sample aged for 700 h. Our previous work [11,14] has proposed that the average size of the LRO phase in the alloy gradually increases with the aging time increasing from 100 h to 500 h. Therefore, it can be concluded that the increase in aging time from 500 h to 700 h can increase the number of the LRO phase but fail to increase significantly the average size of the LRO phase.

A typical of HRTEM image of the alloy aged for 700 h along [001] zone axis is shown in Fig. 4a. The inset is corresponding fast fourier transformation (FFT) diffractogram, which reveals that the LRO phase consists of only one kind of the variant. Fig. 4b also reveals the superlattice reflections of the LRO phase, indicating that the blue boxed region in Fig. 4a can represent the interfacial structure between the LRO phase and the Ni-based matrix. The corresponding inverse fast fourier transformation (IFFT) lattice image (Fig. 4c) reveals an excellent coherent relationship between the LRO phase and the matrix, which is in accordance with the results in Ref. [5,15]. Note that the solution treated sample and the sample aged for 50 h do not contain the LRO phases, due to the absences of the superlattice reflections at $\frac{1}{3}${420} and $\frac{1}{3}${220} positions in their SAED patterns along [001] zone axes. This can be easily explained by the insufficient aging time.

3.2. Tensile properties

3.2.1. Engineering stress–strain curve

The engineering stress–strain curves of different heat-treated samples at room temperature with strain rate of 10^{-3} s^{-1} are presented in Fig. 5a. All the samples exhibit typical continuous yielding. This is because the coarse-grained sample with a less grain boundary area has insignificant change in value of the density and average velocity of mobile dislocations [16]. For the solution treated sample and samples

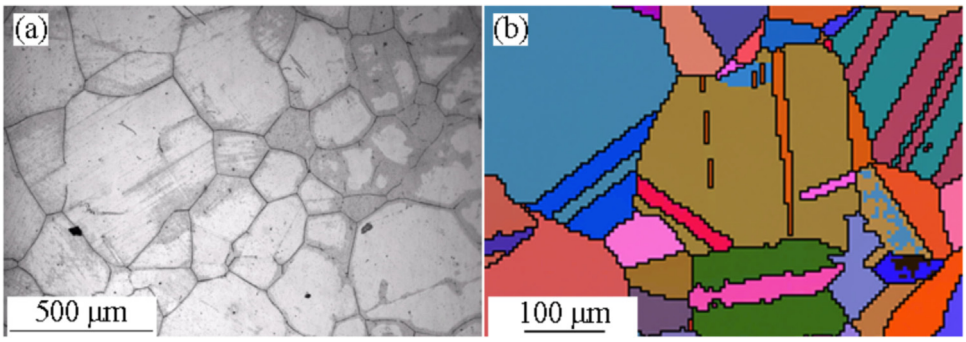

Fig. 2. Optical map (a) and all Euler map (b) of the alloy aged at 600 °C for 500 h. The all Euler map is color-coded according to all Euler orientation.